

## FORMATION OF A CLEARING-UP CHANNEL IN THE CONDENSATION TRACE OF A HIGH-ALTITUDE AIRCRAFT WITH A LASER BEAM

A.V. Kashevarov, M.N. Kogan, A.N. Kucherov, and A.L. Stasenko

*N.E. Zhukovskii Central Aerohydrodynamical Institute, Moscow*

*Received July 29, 1997*

*This paper presents some results of the study of the laser beam propagation in an axisymmetric jet containing the condensing vapor and droplets growing due to collisions. The calculations are made for the flight conditions of the supersonic airliners being under development. Spatial distribution of the condensate mass concentration and droplet size are obtained, as well as the optical characteristics of an aerosol cleared up with a laser beam (e.g., for remote monitoring of gas species in the jet). The fact that evaporation efficiency for a separate droplet and aerosol evaporation parameters depend on droplet size, temperature, droplet substance (water), and other properties of the ambient gas medium, and the intensity of laser radiation vaporizing the droplets is taken into account.*

### INTRODUCTION

A review of papers on the aircraft condensation traces is presented in Ref. 1. The earliest of them appeared in the fiftieths. At present, ecological aspects connected with the design of high-altitude supersonic airliners of the second generation (SSA-2; the first generation includes Tu-144 and Concorde). Model distributions of the turbulent jet parameters (concentration of droplets, carbon dioxide, water vapor; temperature distribution, gas mixture velocity etc.) are presented in Ref. 2. The jet is still hot at the distances up to 100 m from the aircraft nozzle, and its chemical composition differs from that in the atmosphere afterwards. At the distances greater than  $10^3$  m, the vortex sheet from the aircraft starts to interact with the exhaust jets from the engine.<sup>3</sup> At the same time, the structure of the condensation trace and distribution of parameters, including concentration of contaminating species changes significantly. This complicates theoretical and experimental study of the jet.

To investigate the structure, composition of a jet, and concentration of contaminating species (first of all, of nitric oxides and hydroxides), the part of the jet at a distance from  $10^2$  m to  $10^3$  m is most convenient. Use of remote sounding means<sup>4</sup> (in addition to *in situ*<sup>5</sup> sampling) can be hindered by the water aerosol formed.<sup>6</sup> So it is necessary to clear up the condensation jet.

In this paper, the clearing up of the isobaric supersonic condensation trace is studied using numerical calculations of the jet parameters and laser beam, including condensation, coagulation, and evaporation of droplets. The study of the aerosol clearing up is reduced to the water content approximation<sup>7,8,9</sup> on the macroscale on the order of the beam radius,  $r_0$ . Certain specific features of the

evaporation microprocesses in a separate droplet with the radius  $a \ll r_0$  are taken into account. For the initial data at the engine nozzle section we took those that are close to the parameters presented in Ref. 3 (for the American SSA-2) and in Ref. 10 (for the Russian SSA-2).

### 1. PHYSICOMATHEMATICAL MODEL OF THE CONDENSATION TRACE

Let us write the Navier-Stokes equation in cylindrical coordinates  $x, r$  using the boundary layer approximation<sup>11</sup>:

$$\frac{\partial \rho u r}{\partial x} + \frac{\partial \rho v r}{\partial r} = 0;$$

$$\rho u \frac{\partial B}{\partial x} + \rho v \frac{\partial B}{\partial r} = \frac{1}{r} \frac{\partial}{\partial r} \left( r \mu_t \frac{\partial B}{\partial r} \right). \quad (1)$$

Here  $u$  and  $v$  are the components of the jet velocity along the directions  $x$  and  $r$ , respectively;  $\rho$  is the gas density,  $B = (u, J)$ ;  $J$  is the deceleration enthalpy;  $\mu_t$  is the coefficient of turbulent dynamic viscosity. It is accepted that the turbulent Prandtl number  $Pr_t = 1$  in the law of energy conservation. In contrast to Ref. 6, we used the well-known two-parameter,  $k$ - $\epsilon$ , turbulence model in which the distributions of the specific (per unit mass) turbulence energy  $k_t$  and dissipation rate  $e_t$  of turbulent pulsations in a jet are described by the following equations<sup>12</sup>:

$$\rho u \frac{\partial k_t}{\partial x} + \rho v \frac{\partial k_t}{\partial r} = \frac{1}{r} \frac{\partial}{\partial r} \left( r \frac{\mu_t}{C_k} \frac{\partial k_t}{\partial r} \right) + \mu_t \phi - \rho e_t;$$

$$\rho u \frac{\partial e_t}{\partial x} + \rho v \frac{\partial e_t}{\partial r} = \frac{1}{r} \frac{\partial}{\partial r} \left( r \frac{\mu_t}{C_e} \frac{\partial e_t}{\partial r} \right) + (\mu C_1 \phi - \rho C_2 e_t) \frac{e_t}{k_t}. \quad (2)$$

Here  $\mu_t = \rho C_\mu k_t^2 / \epsilon_t$ ;  $\phi = (\partial u / \partial r)^2 + 2(\partial v / \partial r)^2 + 2(v/r)^2$  is the dissipation function; the constants are  $C_k = 1$ ,  $C_e = 1.3$ ,  $C_1 = 1.44$ ,  $C_2 = 1.92$ ,  $C_\mu = 0.09$ . The solution was constructed using the numerical algorithm from Refs. 6 and 11.

To calculate the condensation of water vapor in the jet, we used the equations

$$\begin{aligned} \rho u \frac{\partial Y}{\partial x} + \rho v \frac{\partial Y}{\partial r} &= \frac{1}{r} \frac{\partial}{\partial r} \left( r \frac{\mu_t}{Sc} \frac{\partial Y}{\partial r} \right), \\ \rho u \frac{\partial Y_w}{\partial x} + \rho v \frac{\partial Y_w}{\partial r} &= \frac{1}{r} \frac{\partial}{\partial r} \left( r \frac{\mu_t}{Sc} \frac{\partial Y_w}{\partial r} \right) + \\ &+ 4\pi a^2 \rho n (Y_v - Y_{vs}) \left[ \frac{4}{\alpha_k \langle V \rangle} + \frac{a^2}{D(a+l)} \right]^{-1}, \\ \rho u \frac{\partial (n/\rho)}{\partial x} + \rho v \frac{\partial (n/\rho)}{\partial r} &= \frac{1}{r} \frac{\partial}{\partial r} \left( r \frac{\mu_t}{Sc} \frac{\partial (n/\rho)}{\partial r} \right) - \\ &- 2\pi \sqrt{2} V_t n^2 a^2 \eta_t. \end{aligned} \quad (3)$$

Here  $Y = Y_v + Y_w$  is the sum mass concentration of water vapor,  $Y_v$ , and condensate,  $Y_w$ ;  $a$  is the droplet radius;  $Y_{vs}$  is the concentration of saturated water vapor;  $\alpha_k$  is the condensation coefficient ( $\alpha_k = 1$ );  $\langle V \rangle$  and  $\langle V_v \rangle$  are the average heat velocities of air and vapor molecules, respectively;  $D$  is the coefficient of vapor diffusion;  $n$  is the number concentration of droplets;  $V_t = \sqrt{2k_t}$  is the average rate of turbulent pulsations;  $\eta$  is the coefficient of collisional droplet coagulation;  $l = 2D/\langle V \rangle$  is the mean free path of gas molecules;  $Sc = \mu_t / \rho D_t = 1$  is the Schmidt number;  $D_t$  is the turbulent diffusion coefficient of vapor, droplets, and condensation nuclei. For instance, the characteristic time of the droplet entrainment by gas in a Stokes flow regime has the order of  $\tau = 2a^2 \rho_w / 9\mu_g$  ( $\mu_g$  is the molecular viscosity of the carrier gas) what yields  $\tau \approx 10^{-5}$  s for the radius  $a = 10^{-6}$  m. Such droplets turn to be "frozen" in the gas for turbulent pulsations in a jet at the considered distances from an aircraft. The size of droplets is determined as  $a = (\rho Y_w 3 / 4\pi n \rho_w)^{1/3}$  where  $\rho_w = 10^3$  kg/m<sup>3</sup> is the water density. The second equation in the system (3) takes into account the interpolation formula for droplet growth for arbitrary Knudsen numbers  $Kn = l/2a$ . The formula asymptotically approaches the expressions for the free-molecule and continuous regime at large ( $Kn \gg 1$ ) and small ( $Kn \ll 1$ ) Knudsen numbers, respectively. The last term of the third equation in the system (3) describes the decrease of concentration of droplets formed on the condensation nuclei due to coagulation. To set the coagulation coefficient value  $\eta$ , we used a new theory<sup>13</sup> according to which the processes of condensation or evaporation of droplets are accompanied by attractive or repulsive forces, so the coefficient  $\eta$  can be written in the form

$$\eta = \Omega \phi (Kn) \eta_0; \quad \Omega = \frac{\omega}{1 - \exp(-\omega)};$$

$$\omega = \rho (Y_v - Y_{vs}) a^3 \frac{3\pi}{8m_v},$$

where  $\eta_0$  is the probability of droplet coalescence without the regard of this additional force ( $\eta_0 = 1$ ),  $m_v = 3.0 \cdot 10^{-26}$  kg is the mass of the H<sub>2</sub>O molecule. The theory<sup>13</sup> is valid for the free-molecule regime  $Kn \gg 1$ . As to the continuous regime, additional forces do not appear. So, in this paper we propose an interpolation factor  $\phi(Kn) = [1 + (\Omega - 1) \exp(-Kn)]^{-1}$  asymptotically excluding the additional factor  $\Omega$  for large droplets (for  $Kn \leq 1$ ).

## 2. COMPARISON OF THE ANALYTICAL AND NUMERICAL MODELS FOR COMPUTING THE JET PARAMETERS

The Table I and Figs. 1a and 1B present the condensation jet parameters obtained using the universal Gaussian distribution law as a function of the distance  $x$  from the nozzle and coordinate  $r$  transverse to the axis ( $z = r$  in the coordinate system connected with a beam; we consider the beam intersecting the jet axis). Two Prandtl models of turbulence, I, II, were used (see Eq. (11) in Ref. 6). For a comparison, Ref. 6 presents the parameters at the jet axis (Table I) and distributions along the transverse coordinate (Figs. 1a and 1B) which were obtained numerically in this work (model III). For one of the variants of calculations, we took a data set by American authors<sup>3</sup>: the flight height of an aircraft is approximately 18 km; temperature at the nozzle section is  $T_a = 561$  K, in the ambient air it is  $T_\infty = 216.7$  K; the velocity is  $u_a = 1320$  m/s,  $u_\infty = 708$  m/s; gas mix density is  $\rho_a = 0.0521$  kg/m<sup>3</sup>;  $\rho_\infty = 0.135$  kg/m<sup>3</sup>; relative mole concentration of carbon dioxide is  $C_{CO_2,a} = [(\rho_{CO_2} / \mu_{CO_2}) / (\rho / \mu)]_a = 0.0317$ ;  $C_{CO_2,\infty} = 3.5 \cdot 10^{-4}$ ;  $C_{H_2O,\infty} = 4.4 \cdot 10^{-4}$ ;  $\mu_{CO_2} = 44$  kg/kmole;  $\mu = 29$  kg/kmole;  $\mu_v = \mu_{H_2O} = 18$  kg/kmole; the relative average volume absorption coefficient of CO<sub>2</sub> laser radiation (radiation wavelength is  $\lambda = 10.6$   $\mu$ m) is  $B_w = \alpha_w / \rho_w \approx 10^2$  m<sup>2</sup>/kg; the radius of the engine nozzle is  $r_a = 1$  m. For the Russian variant of the supersonic airliner of the second generation, the following values are accepted<sup>10</sup>:  $T_a = 407$  K,  $\rho_\infty = 216.7$  K;  $\rho_\infty = 0.120$  kg/m<sup>3</sup>;  $u_a = 1000$  m/s;  $u_\infty = 600$  m/s;  $r_a = 0.87$  m;  $C_{H_2O,\infty} = 5.16 \cdot 10^{-3}$ . In both cases, vapor concentration at the nozzle output is taken to be  $C_{H_2O,a} = 0.1$ . (This value is too high for usual fuel, but it is quite realistic for quite promising hydrogen fuel). Let us note the following results of the study. The distributions of velocity  $V/V_0$ , admixture concentration (carbon dioxide etc.) in Fig. 1au curve 3, are close to the Gaussian universal law 1 in near the axis, but they decrease considerably faster in the jet periphery. The distribution of water content (curve 2) satisfactorily coincides with the universal Gaussian law 1.

TABLE I. Comparison of the isobaric condensation jet parameters (at the symmetry axis for  $r = 0$ ) obtained using approximate analytical models I, II<sup>2,6</sup> and numerical model III (this paper). The parameters are as follows: density  $\rho_0$ , temperature  $T_0$ , excess velocity  $V_0$ , water content  $w_*$ , relative mass concentration of carbon dioxide  $Y_{CO_2} = \rho_{CO_2}/\rho$ , absorption coefficients  $\alpha_{CO_2}$ , coefficients of efficient radiation absorption by aerosol  $\alpha_{ew} = (1 - \beta) \alpha_d$  (evaporation efficiency for a separate droplet  $\beta = 0.5$ ), optical thickness  $\tau$ . The distances from the nozzle are  $x = 500$  m and 1000 m.

Distance $x$ , m	500			1000		
Model	I	II	III	I	II	III
$V_0 = u(0) - u_\infty$ , m/s	2.20	15.4	29.14	1.100	9.72	17.52
$T_0$ , K	219	230	241.6	218	225	232
$\rho_0$ , kg/m <sup>3</sup>	0.1335	0.127	0.121	0.134	0.130	0.126
$w_*$ , 10 <sup>-5</sup> kg/m <sup>3</sup>	1.17	8.16	8.46	0.583	5.14	8.53
$Y_{CO_2} \times 10^3$	0.708	1.74	2.49	0.623	1.29	1.58
$\alpha_{CO_2}$ , 10 <sup>-5</sup> m <sup>-1</sup>	1.49	5.45	10.5	1.26	3.43	5.28
$\alpha_{ew}$ , 10 <sup>-3</sup> m <sup>-1</sup>	0.661	4.62	4.55	0.330	2.91	4.27
$\tau$ , 10 <sup>-2</sup>	3.31	8.76	5.12	2.34	6.96	10.2

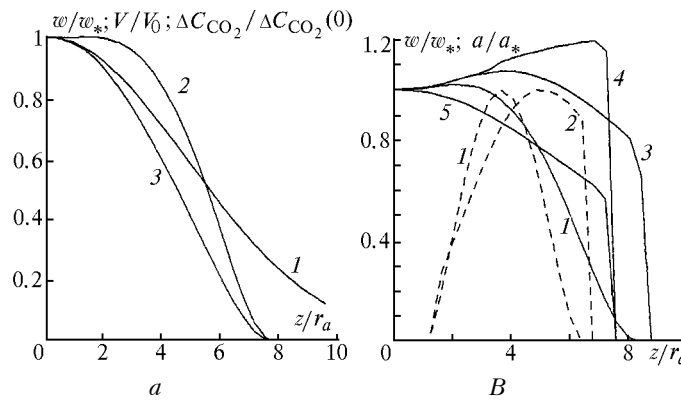


FIG. 1. a) Distributions of the jet parameters at the distance  $x = 1000$  m from the nozzle: universal law<sup>2,6</sup>  $(u - u_\infty)/[(u_a - u_\infty)\epsilon] = (C_{CO_2} - C_{CO_2,\infty})/[(C_{CO_2,a} - C_{CO_2,\infty})\epsilon] = w/w_* = \exp(-z/R_{II}^2)$ ;  $\epsilon = \chi/[R_{II}/r_a]^2 = 0.016$ ;  $\chi = \rho_a u_a / (\rho_\infty u_\infty) = 0.720$ ;  $R_{II} = 6.74$  m;  $r_a = 1$  m (1); water content  $w/w_*$  (III)  $w_* = 8.53 \cdot 10^{-5}$  kg/m<sup>3</sup> (2); relative distributions of the velocity  $V/V_0$  (III) and mole fraction of the carbon dioxide  $C_{CO_2}/\Delta C_{CO_2}(0) = (C_{CO_2}(z) - C_{CO_2,\infty})/[(C_{CO_2}(0) - C_{CO_2,\infty})\epsilon]$  (III) (3). b) Relative distributions of water content  $w/w_*$  (curves 1) and droplet radii (curves 2–5) across the jet at the distance  $x = 500$  m (dashed lines,  $w_* = w_{max} = 8.46 \cdot 10^{-5}$  kg/m<sup>3</sup> (1);  $a_* = a_{max} = 0.850$   $\mu$ m coagulation (2)) and  $x = 1000$  m (solid lines,  $a_* = a_0(0) = 1.271$   $\mu$ m, coagulation (3);  $a_* = a(0) = 0.322$   $\mu$ m, without coagulation (4); Russian SSA–2,  $x = 800$  m,  $r_a = 0.87$  m,  $a_* = a(0) = 3.52$   $\mu$ m, coagulation (5)).

Figure 1b presents the variations of the water content function  $w(z)$  and droplet radii  $a(z)$  in the direction perpendicular to the jet axis at the distance 0.5 km (curve 2) and 1 km (curves 3–5). If the coagulation model used in this paper is not used, i.e., for  $\Omega = 1$ , the size of droplets does not exceed 0.4  $\mu$ m (curve 4); if the improved coagulation model is used, the size increases up to more than 1  $\mu$ m (curve 3). The change of conditions at the nozzle output (Russian SSA–2,<sup>10</sup> curve 5) leads to the growth of droplets up to 7  $\mu$ m in diameter. It is well-known<sup>14,15</sup> that droplets have micron size in clouds. Taking into account coagulation in our experiments,

we obtain that droplet radii are closer to particles' size in clouds. In what follows, we shall show that droplet size play an important role in the process of droplet evaporation and clearing up of the aerosol medium.

### 3. FORMULATION OF THE PROBLEM ON CLEARING UP OF THE CONDENSATION JET

Let us direct a narrow beam ( $r_0/L \ll 1$ ) along the  $z$  axis, across the condensation jet. Radiation propagation is described by the nonlinear equation of paraxial optics<sup>16</sup>:

$$-2 i k_{\lambda} n_0 \frac{\partial E}{\partial z} + \left( \frac{\partial^2}{\partial x^2} + \frac{\partial^2}{\partial y^2} \right) E =$$

$$= k_{\lambda} n_0 \left[ -2k_{\lambda} (n_0 - 1) \frac{\Delta \rho}{\rho_0} + i(\alpha_g + \alpha) \right] E; \quad (4)$$

$$E|_{z=z_0} = E_0(x, y, t) \equiv$$

$$\equiv \begin{cases} \sqrt{I_0} \exp(-(x^2 + y^2)/2r_0^2), & t \geq 0 \\ 0, & t < 0 \end{cases}; E|_{x,y \rightarrow \pm\infty} \rightarrow 0.$$

Here the  $x$  coordinate is directed along the jet axis;  $E$  is the transverse component of the electric field (the radiation intensity is  $I = EE^*$ );  $k_{\lambda} = 2\pi/\lambda$  is the wave number;  $n_0, \rho_0$  are the refractive index and the density of nondisturbed gas medium, respectively;  $i$  is the imaginary unit. In our calculations we took CO<sub>2</sub>-laser radiation at  $\lambda = 10.6 \mu\text{m}$  as a source of radiation evaporating droplets. The coefficient of absorption by gas  $\alpha_g$  is mainly determined by absorption by carbon dioxide. Water vapor and other gases absorb weaker. The coefficient of attenuation by droplets is the integral of the product of the one-droplet absorption cross section by the droplet size-distribution function  $f$  and the droplet concentration  $n$ . The integral is taken over droplet radius 0 to  $\infty$ .<sup>8,14,17</sup>

Droplet evaporation is described by the system of equations

$$a = \frac{da}{dt} = -\frac{j}{\rho_w}; \quad \rho_w C_{pw} \frac{dT}{dt} = \alpha_d I - \frac{3}{a} \{jH + j_t\} \approx 0. \quad (5)$$

Here  $C_{pw}$  and  $H$  are the specific heat and the vaporization heat of water;  $T$  is the droplet temperature;  $I$  is the radiation intensity;  $K_a, \alpha_d = 3K_a(a)/4a$  are the factor and the mean volume coefficient of radiation absorption by a separate droplet. Calculation of the mass and heat fluxes  $j, j_t$  from the droplet surface is described in Ref. 18.

In the jet model considered, the droplet radius  $a$  and functions depending on it are specified by local gas temperature, vapor pressure, and other conditions (e.g., intensity in the evaporation regime), i.e., they are completely defined by coordinates. The function  $f$  is the Dirac delta function  $\delta(a)$ . This is the model of locally monodisperse aerosol. If no droplet size-distribution is added to the jet model accepted, the equation for  $f$  is reduced to the equation for water content  $w \equiv 3/4 \pi a^3 \rho_w n$ :

$$\left( \frac{\partial}{\partial t} + V(z) \frac{\partial}{\partial x} \right) w = -wI \frac{\alpha_d \beta}{\rho_w H},$$

$$w|_{t=0} = w_0(z); \quad w|_{x \rightarrow \infty} \rightarrow w_0(z); \quad (6)$$

$$\beta \equiv \frac{jH}{jH + j_t}; \quad a \equiv \frac{\partial a}{\partial t} = \frac{\alpha_d I \beta a}{3H \rho_w};$$

$$I \equiv \frac{3\{jH + j_t\}}{\alpha_d a} = \frac{3jH}{\alpha_d \beta a}. \quad (7)$$

The efficiency of evaporation  $\beta$  is introduced in terms of which is expressed the droplet evaporation rate. The equations of gas heating under the isobaric approximation ( $\Delta T/T_0 \approx -\Delta\rho/\rho_0$ ) are as follows:

$$\rho C_{p\Sigma} T_0 \left( \frac{\partial}{\partial t} + V(z) \frac{\partial}{\partial x} \right) \frac{\Delta \rho}{\rho_0} = -[\alpha_g + \alpha_{ew}] I;$$

$$\Delta \rho|_{t=0} = 0; \quad \Delta \rho|_{x \rightarrow \infty} \rightarrow 0, \quad (8)$$

where  $C_{p\Sigma}$  is the specific heat of the mixture of vapor and air;  $\alpha_{ew} = (1 - \beta) \alpha_d$ . If one makes the equations (8), (6), and (4) dimensionless, as in Ref. 19, the obtained system includes the following similarity parameters: the Fresnel number  $F = 2\pi r_0^2/\lambda L$  where  $L = 2R$  is the characteristic length of the path,  $R$  is jet radius; the parameters of attenuation by a gas  $N_g = \alpha_g L$  and by the aerosol  $N_B = \alpha_w L/\rho_w$ ; the evaporation (clearing up) parameter  $N_v = \alpha_d I_0 \beta r_0/(\rho_w H_0 V_0)$ ; the parameter of heat self-action  $N = Q(L/r_0)^2(n_0 - 1)/n_0$  where  $Q = \alpha_{ew} I_0 r_0/(\rho_0 C_{p\Sigma} T_0 V_0)$  is the scale of the medium density variation.

#### 4. CLEARING UP RATE AS A FUNCTION OF BEAM PARAMETERS, MEDIUM PARAMETERS, AND DROPLET SIZE

For a correct quantitative description of the clearing up process, one should estimate the evaporation efficiency  $\beta$  for a separate droplet and the parameters  $N_v, N$  depending on it.

At a relatively weak droplet heating, when the surface temperature is  $T_d < T_* = 381-375 \text{ K}$ , ( $a = 1-10 \mu\text{m}$ ), the vapor velocity is small. The diffusion-convective evaporation regime<sup>14,17,18,21</sup> is realized (in the limiting case of very small intensities, the equations of droplet heating (5) are linearized and we can obtain the lower boundary of the evaporation efficiency explicitly<sup>20,21</sup>). Physical properties of water, vapor, and air in the considered range of negative temperatures are presented in Ref. 15. Using Eqs. (5) and (7) and the connection between the mass and heat fluxes  $j, j_t$ ,<sup>18</sup> and intensity, droplet surface temperature, vapor concentration, and other parameters, we obtain the dependence of the clearing up parameters  $N_v$  and self-action  $N$  on the beam parameters  $I_0, r_0$ , medium parameters  $T_0, k_0, p_0$ , droplet material and the initial (characteristic) droplet radius  $a$ . Within the beam scale  $r_0$  and the jet scale  $L$ , the characteristic temperature is the temperature  $T_0$  at the axis.

For a strong heating, when  $T_d < T_*$  and vapor concentration is  $Y_c \approx 1$  (vapor forces out the air), the calculation needs the relations for the jump of parameters at the Knudsen layer<sup>22</sup>  $T_c/T_d = f_t(M_c)$ ,

$\rho_c/\rho_d = f_p(M_c)$ ,  $p_c/p_s(T_d) = f_p(M_c) = f_p f_t$ , and the isentropic relation  $\rho_c/\rho_\infty = 1/[1 + (\gamma - 1)M_c^2/2]^{\gamma/(\gamma-1)}$  (Ref. 18, 23) Taking Mach's numbers  $M_c = u_c/c$  ( $u_c$ ,  $c$  are vapor and sound speed beyond the Knudsen layer) and using the connections between mass and heat flows  $j$ ,  $j_t$ <sup>18</sup> and other parameters, we obtain the dependence of the values  $\beta$ ,  $N_v$ ,  $N$  on the physical parameters of the beam  $I_0$ ,  $r_0$ , of the medium, and droplets in the subsonic regime. Figure 2 presents the evaporation efficiency of an isolated droplet  $\beta$  as a function of the temperature of ambient medium  $T_0$  (Fig. 2a), beam intensity  $I_0$  and droplet radius  $a$  (Fig. 2b), as well as the clearing up parameter  $N_v$  as a function of  $I_0$  and  $a$

(Fig. 2c). To ease a change between the diffusive-convective and subsonic regimes, one should use the iteration procedure.<sup>18</sup> The results significantly differ from those presented in Ref. 14, Fig. 3.6. The fact is that the study in Ref. 14, Chapter 3, Section 3.6, is based on the formula (3.3.16)<sup>14</sup> which is not valid for the diffuse-convective regime. Similar relation is valid not for pressure but relative mass concentrations.<sup>20,21,18</sup> The counterpressure<sup>22</sup> in the subsonic evaporation regime, when the increase of temperature at the droplet surface leads to a decrease of temperature and pressure at the external boundary of the Knudsen layer, is not taken into account in Ref. 14.

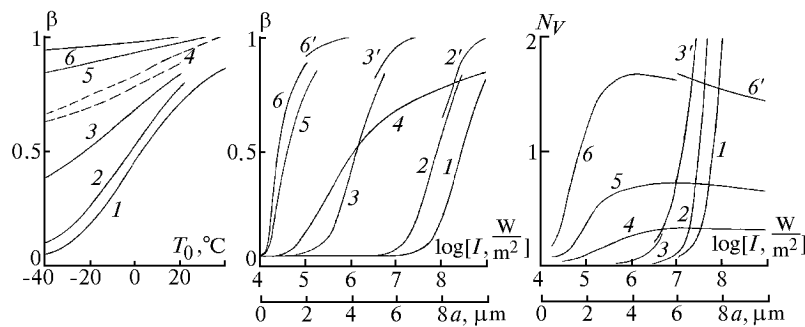


FIG. 2. Evaporation efficiency of an individual droplet  $\beta$  as a function of ambient medium temperature  $T_0$  for different values of intensity  $I$ :  $\beta_{\min}$  for  $I \ll I_*$  (curve 1);  $I = 10^7 \text{ W/m}^2$  (2);  $5 \cdot 10^7 \text{ W/m}^2$  (3);  $10^8 \text{ W/m}^2$  (4), by formulas for the diffusion-convection regime;  $4 \cdot 10^8 \text{ W/m}^2$  (6);  $2 \cdot 10^8 \text{ W/m}^2$  (5);  $10^8 \text{ W/m}^2$  by formulas for the subsonic regime (4). Droplet radius  $a = 1 \mu\text{m}$  (a). Evaporation efficiency as a function of radiation intensity  $I$  ( $a = 0.5 \mu\text{m}$  (1);  $1 \mu\text{m}$  (2);  $10 \mu\text{m}$  (3)) and the initial (characteristic) droplet radius ( $I = 5.3 \cdot 10^6 \text{ W/m}^2$  (4);  $5.3 \cdot 10^7 \text{ W/m}^2$  (5);  $10^8 \text{ W/m}^2$  (6)). Curves 2', 3', 6' show the calculations by formulas for the subsonic regime. Temperature  $T_0 = 233 \text{ K}$  (b). The clearing up parameter  $N_v$  as a function of intensity  $I$  ( $a = 0.5 \mu\text{m}$  (1);  $1 \mu\text{m}$  (2);  $10 \mu\text{m}$  (3)) and the initial droplet radius  $a$  ( $I = 5.3 \cdot 10^6 \text{ W/m}^2$  (4);  $I = 10^7 \text{ W/m}^2$  (5);  $I = 2 \cdot 10^7 \text{ W/m}^2$  (6))x Curves 3', 6' are obtained by formulas for the subsonic regime (c).

**5. THE RESULTS OF CALCULATIONS OF THE JET CLEARING UP**

As was demonstrated above, the clearing up parameter  $N_v$  significantly depends on the aerosol microstructure (droplet radius  $a$ ), beam power  $P_0 = I_0 \pi r_0^2$  and radius  $r_0$ , on the physical parameters of a gas jet (temperature, velocity) because the evaporation efficiency  $\beta$  depends on these values. The calculations of the clearing up process of the condensation jet for input data close to Ref. 3 (see item 2) were performed with the allowance for the established dependences. The procedure of solving the system of equations (4), (6), and (8) is described in Ref. 19. The results of our experiment are presented in Figs. 3 and 4. The values of the heat self-action parameter  $N$  are small in the considered range of physical parameters of the beam and medium.

As a rule, the Fresnel number is large,  $F \gg 1$ . For the case of a parallel beam of radius  $r_0 = 0.05 \text{ m}$ , the diffraction blurring begins to have an effect with the displacement of a source at the distance

$L_1 \leq 1.5 \text{ km}$ . For  $L_1 \approx 10 \text{ km}$ , one should use a focusing mirror in order to obtain a beam of the required radius  $r_0$  at the jet location. The minimum radius of the focusing mirror  $r_1$  can be estimated by the expression for the halfangle of the diffraction divergence  $\vartheta \approx 0.61\lambda/r_0$ :  $r_1 \approx L\vartheta = 0.61\lambda L/r_0 \approx 1.29 \text{ m}$  ( $L = 10^4 \text{ m}$ ;  $\lambda = 10.6 \mu\text{m}$ ;  $r_0 = 0.05 \text{ m}$ ). The convergence angle of a non-disturbed beam is so small that the beam can be treated as a parallel one at the length of the cross dimension of the jet  $L \approx 10 \text{ m}$ ; the phase front can be considered to be flat when entering the jet.

The water content functions and optical thickness of an undisturbed and cleared up jet along the beam path at the distance  $x = 1000 \text{ m}$  are constructed in Fig. 3a; Fig. 3b presents similar dependences obtained for the distance  $x = 500 \text{ m}$  from the nozzle (the model of Ref. 6). In the latter case, the aerosol has not yet filled the central near-axis part of the jet. A small dip at the jet axis in the initial water content distribution, not yet disturbed by a laser beam, is observed also at the distance  $1000 \text{ m}$ .

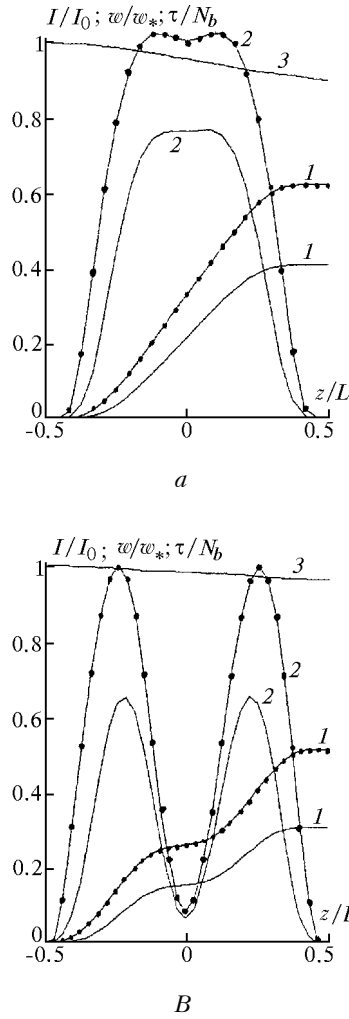


FIG. 3. a) Distributions of the parameters across the condensation jet at the axis of the incident beam; in the section  $x = 1000$  m: optical thickness  $\tau/N_B$  (1); water content  $w/w_0$  (2); intensity  $I/I_0$  (3). Physical parameters are as follows: beam radius  $r_0 = 0.05$  m, intensity  $I_0 = 2 \cdot 10^7$  W/m<sup>2</sup> ( $\beta = 0.143$  for  $a = 1$   $\mu$ m), water content  $w_* = 8.53 \cdot 10^{-5}$  kg/m<sup>3</sup>, velocity  $V_0 = 17.5$  m/s;  $-\bullet-\bullet-$  for  $t = 0$ ;  $-----$  for  $t = 5t_0$ ;  $t_0 = 0.00285$  s. Similarity parameters:  $N_B = 0.164$ ;  $N_v = 0.314$ ;  $N = 0$ ;  $F \gg 1$ . B) Section  $x = 500$  m (without allowance for coagulation<sup>6</sup>):  $r_0 = 0.05$  m;  $I_0 = 1.75 \cdot 10^7$  W/m<sup>2</sup>, ( $\beta = 0.120$  for  $a = 1$   $\mu$ m);  $V_0 = 23.8$  m/s;  $w_* = 2.62 \cdot 10^{-5}$  kg/m<sup>3</sup>;  $N_B = 0.034$ ;  $N_v = 0.224$ ;  $N = 0$ ;  $F \gg 1$ .

Figure 4 presents the water content and optical thickness (at the jet axis and at the far end of the beam from the radiation source) as functions of the clearing up parameter  $N_v$  and beam power  $P_0$ . The functions of  $N_v$  and  $P_0$  significantly differ even for small  $N_v$ . Comparison of the numerical solution of the system of equations (4), (6), and (8) with the analytical Glickler solution<sup>7-9,14,17,19</sup> (for a homogeneous transverse wind

$V_{00} = V_0(z = L/2)$  demonstrates that water content values in fact coincide with the numerical ones. Optical thickness differs by its value at  $N_v \geq 1$ .

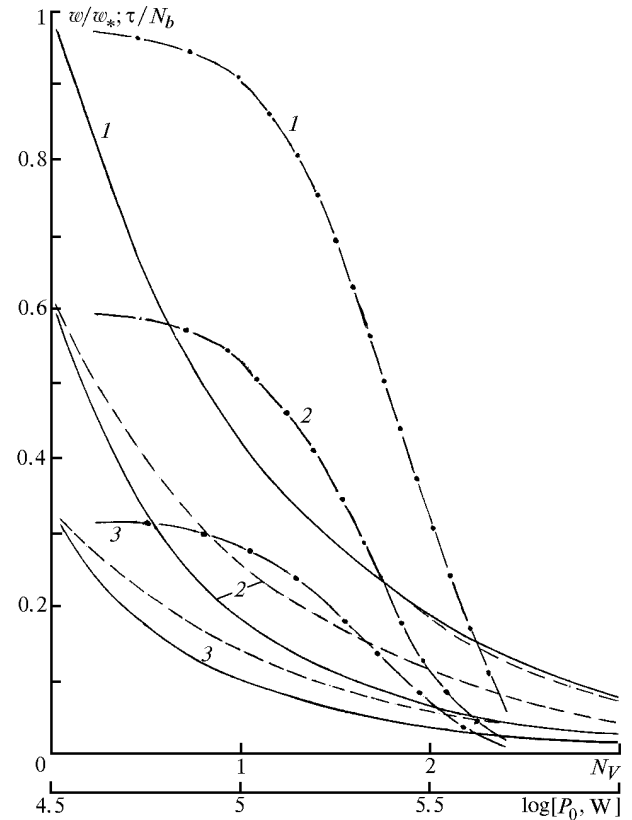


FIG. 4. Water content  $w/w_*$  in the jet at the symmetry axis  $z = 0$  (curves 1) and optical thickness  $\tau/N_B$  in the center of the jet (curves 3) and at its edge (curves 2) as functions of the clearing up parameter  $N_v$ . The dashed lines show the analytical solution. Similar functions  $w/w_*$ ,  $\tau/N_B$  of power  $P_0$  are shown by dot-and-dash lines. The parameters are as follows:  $r_0 = 0.05$  m;  $V_0 = 17.5$  m/s;  $w_* = 8.53 \cdot 10^{-5}$  kg/m<sup>3</sup>;  $N_B = 0.164$ ;  $N = 0$ ;  $F \gg 1$ .

ACKNOWLEDGMENT

The work is supported by MNTTs (project No. 200) and the Russian Foundation for Basic Research (ANK).

REFERENCES

1. I.P. Mazin, *Izv. RAN, Fiz. Atmos. Okeana* **32**, No. 1, 5–18 (1996).
2. A.L. Stasenko, "Contribution to the theory of nitric oxides chemisorption by water droplets in the jet of a stratospheric aircraft," Preprint No. 51, N.E. Zhukovskii Central Aerohydrodynamical Institute, Moscow (1991), 36 pp.

3. R.C. Miake-Lye, M. Martinez-Sanchez, R.C. Brown, and C.E. Kolb, *J. Aircraft* **30**, No. 4, 467–479 (1993).
4. R.M. Measures, *Laser Remote Sensing* (John Wiley and Sons, New York, 1987).
5. D.W. Fahey, E.R. Keim, et al., *Science* **270**, No. 5232, 70–74 (1995).
6. A.V. Kashevarov and A.L. Stasenko, *Uchen. Zap. TsAGI* **25**, No. 3–4, 105–116 (1994).
7. S.L. Glickler, *Applied Optics* **10**, No. 3, 644–650 (1971).
8. A.P. Sukhorukov and E.N. Shumilov, *Zh. Tekh. Fiz.* **43**, No. 5, 1029–1041 (1973).
9. G.W. Sutton, *Applied Optics* **17**, No. 21, 3424–3430 (1978).
10. L.E. Vasil'ev, S.I. Popov, and G.P. Svishchev, *Tekh. Vozd. Flota*, No. 1–2, 14–17 (1994).
11. V.A. Ruskol and U.G. Pirumov, *Dokl. Akad. Nauk SSSR* **246**, No. 2, 321–324 (1977).
12. V.S. Avduevskii, D.A. Ashratov, A.V. Ivanov, and U.G. Pirumov, *Supersonic Non-Isobaric Gas Jets* (Mashinostroenie, Moscow, 1985), 248 pp.
13. C. Cercignani, A. Frezzotti, and M.N. Kogan, *Physics of Fluids* **A5**, No. 10, 2551–2556 (1993).
14. O.A. Volkovitskii, Yu.S. Sedunov, and L.P. Semenov, *Propagation of Intense Laser Radiation in Clouds* (Gidrometeoizdat, Leningrad, 1982), 312 pp.
15. I.P. Mazin and S.M. Shmeter, *Clouds: Structure and Physics of Their Formation* (Gidrometeoizdat, Leningrad, 1983), 280 pp.
16. M.B. Vinogradova, O.V. Rudenko, and A.P. Sukhorukov, *Wave Theory* (Nauka, Moscow, 1979), 384 pp.
17. V.E. Zuev, A.A. Zemlyanov, Yu.D. Kopytin, and A.V. Kuzikovskii, *Powerful Laser Radiation in the Atmospheric Aerosol* (Nauka, Novosibirsk, 1984), 223 pp.
18. A.N. Kucherov, *Teplofiz. Vys. Temp.* **29**, No. 1, 144–152 (1991).
19. A.N. Kucherov, *Kvant. Elektron.* **22**, No. 3, 253–257 (1995).
20. F.A. Williams, *Intern. J. of Heat and Mass Transfer* **8**, No. 4, 575–590 (1965).
21. R.L. Armstrong, *Appl. Optics* **23**, No. 1, 148–155 (1984).
22. C.J. Knight, *AIAA J.* **17**, No. 5, 519–523 (1979).
23. A.V. Butkovskii, *Inzh.-Fiz. Zh.* **58**, No. 2, 318 (1990) (Dep VINITI No. 6023–B89).